

- (18) T. K. Devon and A. I. Scott, "Handbook of Naturally Occurring Compounds", Vol. II, "Terpenes", Academic Press, New York, N.Y., 1972, p 55.
- (19) T. W. Bentley, R. A. W. Johnstone, and J. Grimshaw, *J. Chem. Soc. C*, 2234 (1967).
- (20) H. Inouye, S. Veda, and Y. Nakamura, *Tetrahedron Lett.*, 5229 (1966).
- (21) A. A. Qureshi and A. I. Scott, *Chem. Commun.*, 948 (1968).
- (22) A. R. Battersby, J. C. Byne, R. S. Kopil, J. A. Martin, T. G. Payne, D. Arigoni, and P. Loew, *Chem. Commun.*, 951 (1968).
- (23) A. R. Battersby, *Pure Appl. Chem.*, 14, 117 (1967).
- (24) A. R. Battersby, A. R. Burnett, and P. G. Parsons, *J. Chem. Soc. C*, 1187 (1969).
- (25) A. R. Battersby, A. R. Burnett, and P. G. Parsons, *J. Chem. Soc. C*, 1277 (1968).
- (26) R. Guarracia, L. Botta, and C. J. Coscia, *J. Am. Chem. Soc.*, 96, 7079 (1974).
- (27) H. Inouye, T. Yoshida, S. Tobita, K. Tanaka, and T. Nishioka, *Tetrahedron*, 30, 201 (1974).

## Flow Nuclear Magnetic Resonance Study of the Dehydration of the Tetrahedral Intermediate Resulting from the Addition of Hydroxylamine to Acetaldehyde<sup>†</sup>

Michael Cocivera,\* Colin A. Fyfe, Adan Effio, Shiv P. Vaish, and Holger E. Chen

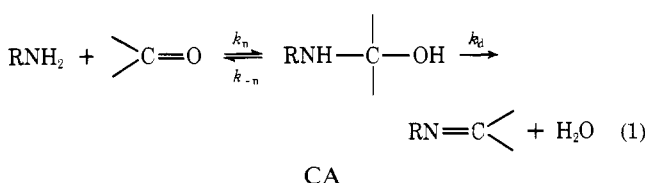
Contribution from the Guelph-Waterloo Centre for Graduate Work in Chemistry, University of Guelph, Guelph, Ontario, N1G 2W1 Canada.

Received June 13, 1975

**Abstract:** The tetrahedral intermediate resulting from the nucleophilic addition of hydroxylamine to acetaldehyde in aqueous solution has been detected by means of NMR using flowing liquids. The rate of dehydration of the intermediate was measured as a function of pH and buffer concentration at 30°C. In addition, the rates of formation of syn and anti oximes were measured under the same conditions. It was found that the rate of dehydration of the intermediate is general acid catalyzed. The rate of appearance of the syn and anti oximes equals the rate of disappearance of the intermediate. However, the rate of formation of syn oxime is slower than the rate for the anti oxime. In addition, the rate of equilibration of syn and anti isomers is catalyzed by the buffer. The values for the rate constants for the various processes will be presented, and details of dehydration of the intermediate and equilibration of syn and anti oximes are discussed.

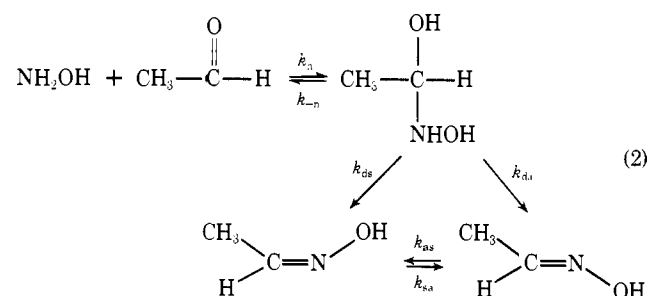
### Introduction

Kinetic studies of the addition of nitrogen nucleophiles to carbonyl compounds have been made by a number of workers.<sup>1-4</sup> The kinetic evidence supports strongly the conclusion that the reaction proceeds according to the mechanism



in which  $k_n$  is the rate constant for nucleophilic addition and  $k_d$  is the rate constant for dehydration of the carbinolamine CA. According to this mechanism, the carbinolamine CA is an intermediate. In many of these studies, the kinetic measurements were made using uv-visible spectroscopy, and the spectrum of the carbinolamine was not observed.<sup>5</sup> Consequently, a detailed kinetic study of the dehydration step by direct observation of the decay of the carbinolamine intermediate has not been made. For this reason, we have undertaken a study of the nucleophilic addition of hydroxylamine to acetaldehyde using the nuclear magnetic resonance spectroscopy (NMR) of flowing liquids.<sup>6</sup> In this paper, we report part of the NMR spectrum of the carbinolamine intermediate and the measurement of its decay, as

well as the growth of the oxime at a number of pH values and buffer concentrations for various buffers. The results can be discussed in terms of mechanism 2, in which the dehydration step involves the formation of the syn ( $k_{ds}$ ) and the anti ( $k_{da}$ ) isomers under kinetic controlled conditions,



followed by equilibration. Thus, our technique permits the direct observation of the properties of the intermediate and the various forms of the product.

### Experimental Section

Flow NMR measurements were made using a suitably modified HA 100 spectrometer of which a detailed description will be given in a forthcoming publication.<sup>7</sup>

In brief, a system is used which includes two reservoirs to permit the protons of one or both of the reacting solutions to come to equilibrium in the applied magnetic field prior to mixing. Equal volumes are mixed in a high-pressure mixing chamber and flowed continuously through the measuring coils of the probe. There is some line broadening as a function of the flow rate, but at suitable flow rates the signal/noise ratio is appreciably better than for a stationary sample, as the nuclei are not saturated as readily by the

<sup>†</sup> Presented in part at the 167th National Meeting of the American Chemical Society, Los Angeles, Calif., 1974, the International Symposium on Nucleophilic Substitution, Mt. Pocono, Penna., 1975, and the 16th Experimental NMR Conference in Asilomar, Calif., 1975.

\* Author to whom correspondence should be addressed.

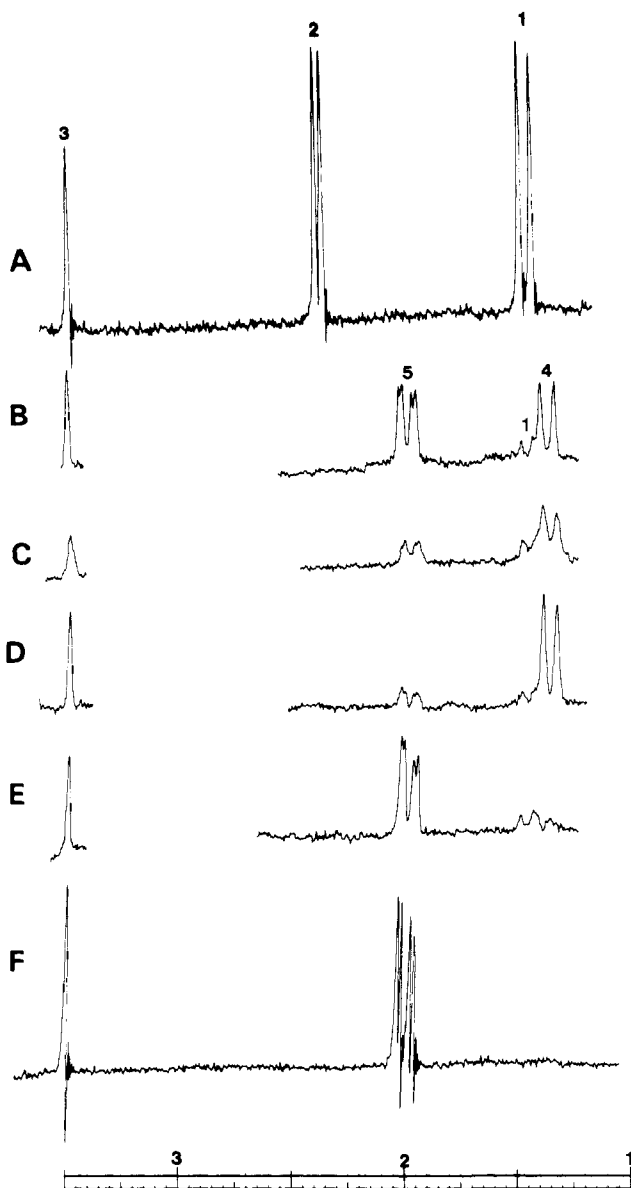


**Figure 1.** Proton nuclear magnetic resonance spectra at 100 MHz and room temperature without spinning. All spectra were obtained at 500-Hz sweepwidth, and the scale at the bottom indicates ppm with the field strength increasing from left to right. In each case, only the portion of the spectrum occurring at higher field strength than the  $\text{H}_2\text{O}$  lock signal is illustrated. All solutions contain methanol for reference. (A) Static 0.2 *M* acetaldehyde solution at pH 7.1; (B) flowing at 10 ml/min after mixing 0.2 *M* acetaldehyde with 0.4 *M* hydroxylamine at pH 7.1; (C) same as B except the flow rate is 26 ml/min; (D) same as B except pH is 8.0; (E) same as B except pH is 6.5; (F) static after mixing at pH 7.1.

irradiating field. The capacity of the reservoirs imposes a limitation on both the flow rate and the length of time the flow can be continued. This can be maximized by using a probe design in which the transmitter-receiver coupling is minimized by time-sharing techniques<sup>8</sup> and the space occupied by the balance "paddles" in the usual probe design is made available.

Chemicals used were from commercial sources and were purified by literature methods to make melting points and spectroscopic properties consistent with those previously reported. All aqueous solutions for rate measurements were prepared at an ionic strength of 1.6 (KCl) except for the boric acid solutions which were at an ionic strength of 1.6 and 0.5. The pH's of the solutions were measured using a Radiometer PHM 63 digital pH meter and are reported to  $\pm 0.02$  unit. The pH of the reaction mixture was measured as a function of time at 5-sec intervals immediately after mixing. The value of  $\text{p}K_a'$  for each buffer was measured by potentiometric titration. The temperature for all determinations was  $30 \pm 0.3^\circ\text{C}$ .

## Results

Mixing an aqueous solution of 0.3 *M* acetaldehyde with an equal volume of an aqueous solution of 0.4 *M* hydroxylamine<sup>14</sup> results in the formation of a carbinolamine that is unstable and undergoes dehydration to form the syn and anti oximes under the conditions employed. The detection of the NMR spectrum of the carbinolamine is possible by flowing the liquid through the probe of the spectrometer. The spectra given in Figure 1 were used to assign the  $\text{CH}_3$  proton resonance of the carbinolamine. This figure, which illustrates spectra obtained under static and flowing conditions, presents only those signals that occur at higher field strength than the  $\text{H}_2\text{O}$  lock signal. Field strength increases from left to right. Figure 1A is due to a static acetaldehyde solution at pH 7.1 without spinning using a 500-Hz sweepwidth. The assignments in order of decreasing field strength are methyl hydrogen (doublet, 1) of the hydrate of acetaldehyde, methyl hydrogen (doublet, 2) of acetaldehyde, and methyl hydrogen (singlet, 3) of methanol which is added for reference. The carbonyl hydrogen (quartet) was clearly resolved at lower field; however, the methine hydrogen of the hydrate is lost in the  $\text{H}_2\text{O}$  resonance. Except for line broadening, the spectrum obtained when this solution is flowing is identical with the static spectrum. The static spectrum of the hydroxylamine solution is not illustrated because the resonances for this compound could not be observed, presumably because of proton exchange with water.

Figures 1B and 1C illustrate the spectra obtained during flowing when these solutions are mixed at pH 7.1. The methyl doublet (2) of acetaldehyde is not observed. In addition to the resonance of methanol (3) and the weak resonance of the hydrate (1), new resonances due to three additional compounds are observed, and the intensities (but not the positions relative to methanol) of these resonances depend on the flow rate, as can be seen by comparing Figure 1B (flow rate, 10 ml/min) with Figure 1C (flow rate, 26 ml/min). Assignments of these new resonances are based on their positions and multiplicities, as well as their behavior during and after flowing. Thus, the high-field doublet (4) is assigned to the  $\text{CH}_3$  resonance of the carbinolamine intermediate  $\text{CH}_3\text{CH}(\text{OH})\text{NHOH}$  because it is a doublet and has a chemical shift at about the same field strength as the methyl resonance of the hydrate of acetaldehyde, and also because its intensity decays to zero after the flow is stopped, as can be seen in Figure 1F. For three reasons we have ruled out the possibility that this doublet is due to the hydrate. First, the chemical shift relative to methanol (3) for the weaker doublet (labeled 1) in Figure 1B is identical with the chemical shift measured for the hydrate from Figure 1A. Second, as the concentration of aldehyde plus hydrate is increased relative to the hydroxylamine, the intensity of the weaker doublet increases when flow rate is constant. Third, if an excess of aldehyde plus hydrate is used, the doublet labeled 1 in Figure 1B remains after the flow is stopped.<sup>15</sup> For these reasons, the assignments given above seem valid. In addition to the methyl resonance, the intermediate should exhibit resonances due to the methine hydrogen and the amino hydrogen. Neither of these has been observed, presumably because the methine resonance occurs close to the  $\text{H}_2\text{O}$  resonance and the amino hydrogen is exchanging with the  $\text{H}_2\text{O}$  hydrogen.

The signals labeled 5 in Figure 1B consist of two doublets that have been assigned to the methyl resonances of the syn and anti isomers of the product oxime  $\text{CH}_3\text{CH}=\text{NOH}$ . The assignment of the syn and anti signals is based on the results of Karabatsos.<sup>9</sup> As expected, the intensities of these product signals increase after the flow is stopped, as can be seen in Figure 1F. In addition, after the flow is stopped, the

## 0.4M Phos, pH 7.7

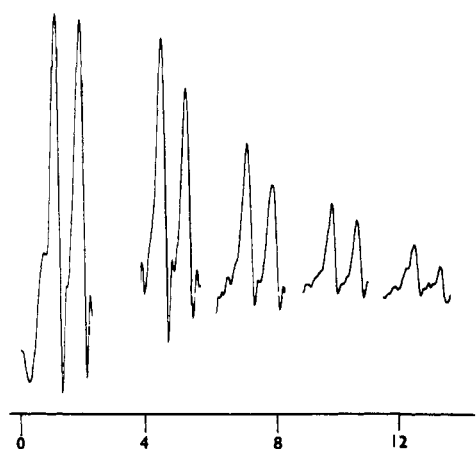


Figure 2. Time dependence (in seconds) of the intensity of the  $\text{CH}_3$  doublet of the carbinolamine  $\text{CH}_3\text{CH}(\text{OH})\text{NHOH}$  after flow is stopped. The buffer concentration and pH are as indicated.

two quartets due to the vinyl hydrogen of the syn and anti oxime are observed at lower field strength.

As can be seen by comparison of Figure 1B with Figure 1C, when the flow rate is increased, the intensity of the doublet 4 due to the carbinolamine increases relative to the intensities of the doublets 5 of the syn and anti oximes. This behavior is to be expected if our assignments are correct since, according to eq 1, the carbinolamine intermediate undergoes dehydration to form the oxime. Thus as the flow rate increases, the time between mixing and measurement is reduced, and the concentration of the carbinolamine should increase while less oxime should be formed.

The spectra illustrated in Figures 1E, 1B, and 1D were measured at pH 6.5, 7.1, and 8.0, respectively, and a flow rate of 10 ml/min. Comparison of these spectra indicate, on a qualitative basis, that the dehydration step is rate determining since the carbinolamine doublet 4 is observed, whereas the aldehyde doublet 2 is not. Furthermore the dehydration step appears to be acid catalyzed since the decay rate of doublet 4 decreases as the pH of the solution is increased. This can be seen in the increase in the intensity of doublet 4 relative to 5 as the pH is increased.

These qualitative observations have been made more quantitative by measurement of the rates of decay of the carbinolamine and growth of the syn and anti oximes using a variety of buffers and pH values. All of the measurements were made at a thermostated temperature of  $30^\circ\text{C}$ . For each buffer at each pH value, the rates were measured at various buffer concentrations. The rates were determined by measuring the intensity of a signal as a function of time after the flow had been stopped. For the present work, this approach permitted the measurement of the decay kinetics of the carbinolamine when its lifetime was as short as 8 sec.

Examples of the intensity vs. time measurements are illustrated in Figures 2 and 3. Figure 2 illustrates the time dependence of the  $\text{CH}_3$ -proton doublet 4 of the carbinolamine for a solution containing 0.4 M phosphate buffer at pH 7.70. Under these conditions, the lifetime of the intermediate is 8 sec. At the beginning of the first scan, a small fraction of the acetaldehyde hydrate is still present. By the start of the second scan, the hydrate signal intensity is negligible compared with the carbinolamine signal intensity. Thus at this point, conversion of the hydrate to the carbinolamine is virtually complete, and the decay of the carbinolamine is first order. At higher pH values, the conversion of the hydrate to the carbinolamine is more rapid and the

0.4M DABCO pH 8.0

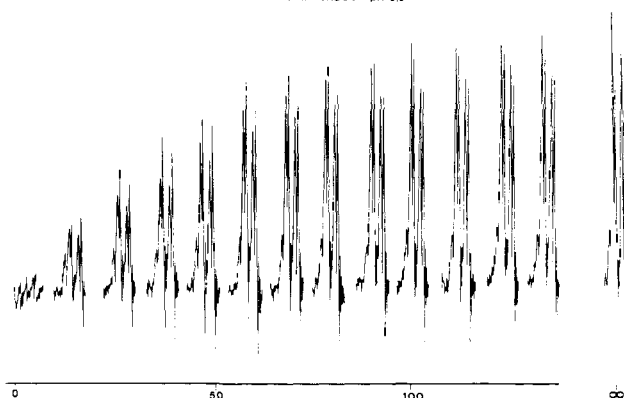


Figure 3. Time dependence of the intensity of the  $\text{CH}_3$  doublets for the syn and anti oximes after the flow is stopped, for 0.4 M Dabco at pH 8.00. The times are in seconds.

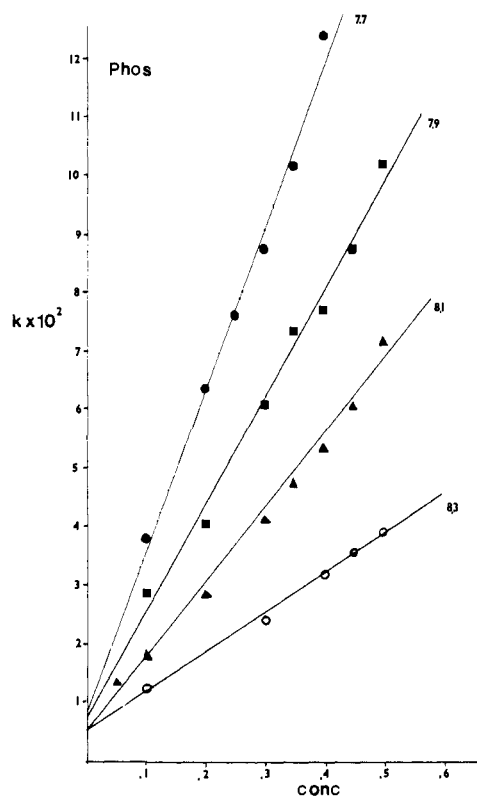


Figure 4. Plots of  $k_{\text{obsd}}$  vs. total phosphate concentration at pH values indicated. The values for  $k_{\text{obsd}}$  are obtained from the first-order decay of the carbinolamine.

hydrate signal is not observed. In addition, the first-order decay of the carbinolamine decreases with increasing pH and more data points can be collected.

Figure 3 illustrates the time dependence for the intensities of the  $\text{CH}_3$  doublets (5) due to the syn and anti isomers of the oxime. This measurement, which was made using 0.4 M Dabco at a pH value of 8.50, was chosen to illustrate the growth of the oxime and the equilibration of its syn and anti isomers. From this figure, it is clear that the ratio, syn:anti, obtained from the dehydration step differs from the equilibrium ratio.

These measurements for the intermediate and the oximes were made using Dabco, phosphate, imidazole, and boric acid as catalysts. The observed first-order rate constants were determined at various pH values and various concentrations of catalyst. Figure 4 illustrates plots of  $k_{\text{obsd}}$  (for

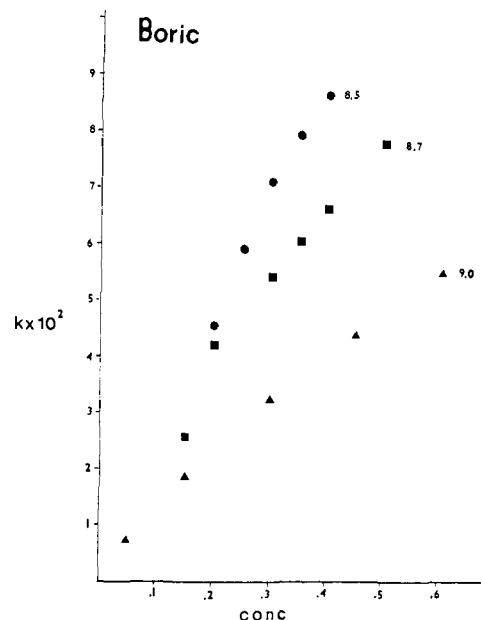


Figure 5. Plots of  $k_{\text{obsd}}$  vs. the total concentration of boric acid at the pH values indicated. The values for  $k_{\text{obsd}}$  are obtained from the first-order decay of the carbinolamine.

decay of the intermediate) as a function of total phosphate concentration at the pH values indicated. Each point is an average of at least four determinations. Similar linear dependence was observed when Dabco or imidazole were used, although the catalytic effects were smaller. For the phosphate catalysts, there was a rapid initial drop of about 0.2 pH unit upon mixing. However, after this initial change, the pH remained constant during the reaction. This change in pH was very rapid relative to the decay rate of the carbinolamine. Consequently, the carbinolamine decay occurred under conditions of constant pH at the values indicated. For the other catalysts, except boric acid, no pH change occurred upon mixing. The situation is different for boric acid. For this catalyst, there is a rapid initial change in pH followed by a gradual change on the same time scale as the decay of carbinolamine. In the course of the reaction, the pH went through a minimum (about 0.6 pH unit below the initial value) and returned to the initial value by the end of the reaction. Nevertheless, the decay of the intermediate is first order under these conditions. However, a nonlinear dependence of the pseudo-first-order rate constant on boric acid concentration is observed, as indicated in Figure 5.

The lines indicated in Figure 4 are least-squares fits of the data. The slopes and the intercepts obtained from this analysis are listed in Table I for phosphate and the other catalysts employed. In addition, the value for the general acid catalytic rate constant  $k_{\text{GA}}$  is given in this table. The value for  $k_{\text{GA}}$  has been determined properly for only the phosphate catalyst, for which there are data at several pH values. For this catalyst, general base catalysis of the dehydration step was found to be negligible. The values of  $k_{\text{GA}}$  for Dabco and imidazole were calculated assuming negligible general base catalysis. These values were used to ascertain the value of the intercept  $k_0$  at the pH values for which only one concentration of Dabco or imidazole was used. This approach seems reasonable since the catalytic effects of these catalysts were not large.

The rate constants for the formation of the syn and anti isomers were determined for each catalyst at various pH values and concentrations. In general, while the absolute values for these rate constants are dependent on the concentration of catalyst, the relative values for syn vs. anti are

Table I. Slopes and Intercepts from Plots of  $k_{\text{obsd}}$  vs. Total Buffer Concentration at 30°C

Buffer	pK <sub>a</sub> <sup>a</sup>	pH	Concn range, M <sup>b</sup>	Fraction acid <sup>c</sup>	$k_0^d \times 10^3 \text{ sec}^{-1}$	Slope <sup>e</sup> $\times 10^2 \text{ M}^{-1} \text{ sec}^{-1}$	$k_{\text{GA}}, \text{ M}^{-1} \text{ sec}^{-1}$
Phosphate	6.37	8.30	0.1–0.5	0.012	5.1	6.76	
		8.10	0.05–0.5	0.018	5.0	12.4	5.76 <sup>f</sup>
		7.90	0.1–0.5	0.029	7.5	18.1	
Dabco	9.24	7.70	0.1–0.5	0.045	7.7	27.7	
		9.00	0.40	0.63	6.8 <sup>g</sup>		
		8.50	0.30	0.85	8.3 <sup>g</sup>		
Imidazole	7.24	8.00	0.1–0.4	0.95	16.6	0.60	0.0064 <sup>h</sup>
		7.70	0.1–0.4	0.26	19.8	4.95	0.19 <sup>h</sup>
		8.10	0.4	0.12	10.1 <sup>g</sup>		
Hydroxylamine	6.15	8.70	0.4	0.034	6.1 <sup>g</sup>		
		7.70	0.1–0.5	0.028		0.6	0.21 <sup>h</sup>

<sup>a</sup> Ionic strength 1.60 (KCl). <sup>b</sup> Total concentration of buffer, including all states of protonation. <sup>c</sup> Fraction of buffer in the acid form. <sup>d</sup> Intercept obtained from a linear least-squares fit of  $k_{\text{obsd}}$  vs. total buffer concentration. <sup>e</sup> From linear least-squares fit of  $k_{\text{obsd}}$  vs. total buffer concentration. <sup>f</sup> Obtained from a plot of slope (column 7) vs. fraction acid (column 5). <sup>g</sup> Assuming  $k_{\text{GA}}$  has the indicated value. <sup>h</sup> Assuming general base catalysis is negligible (see text).

Table II. Rate Constants for the Dehydration Step at 30°C in H<sub>2</sub>O

Catalyst	pH	Concn, <sup>a</sup> M	$k_{\text{obsd}} \times 10^2 \text{ sec}^{-1}$	
			CA <sup>b</sup>	Oxime <sup>c</sup>
Phosphate	7.70	0.20	6.21	5.60
	7.90	0.30	6.04	5.30
	8.10	0.30	4.12	4.60
Dabco	8.00	0.30	1.73	1.53
	8.50	0.30	0.827	0.778
Imidazole	7.70	0.20	3.05	2.64

<sup>a</sup> Total buffer concentration, including all states of protonation. <sup>b</sup> Obtain from the decay rate of the carbinolamine. <sup>c</sup> Obtain from the growth rate of the syn and anti oxime.

not. The absolute values of first-order rate constants for oxime growth for a limited number of catalyst concentrations and pH values are listed in Table II along with the first-order rate constant determined from the decay of the carbinolamine. Comparison of the two columns indicates that the rate constants for the carbinolamine have values that are within about 10% of those for the oxime. The relative rates for syn vs. anti growth  $k_{\text{ds}}/k_{\text{da}}$  via the dehydration step are indicated in Table III. For all the catalysts, except Dabco,  $k_{\text{ds}}/k_{\text{da}}$  is obtained from the ratio, syn:anti, after the dehydration step is completed. This approach is possible because the rate of equilibration of syn and anti isomers is slow relative to the rate of dehydration for these catalysts. For boric acid, phosphate, and imidazole, the absolute values for  $k_{\text{da}}$  and  $k_{\text{ds}}$  at each pH and catalyst concentration can be calculated using these ratios and the expression,  $k_{\text{obsd}} = k_{\text{da}} + k_{\text{ds}}$ , in which  $k_{\text{obsd}}$  is the first-order rate constant determined from carbinolamine decay or oxime growth.

For Dabco, the rate of equilibration is comparable to the rate of dehydration. As a result,  $k_{\text{ds}}$  and  $k_{\text{da}}$  were obtained by fitting the equation

$$\frac{S - S_{\infty}}{S_{\infty} + A_{\infty}} = B \exp[-(k_{\text{ds}} + k_{\text{da}})t] - \left( \frac{S_{\infty}}{S_{\infty} + A_{\infty}} + B \right) \exp[-(k_{\text{as}} + k_{\text{sa}})t] \quad (3)$$

to the time dependence of the syn NMR signal intensities

**Table III.** Relative Rate Constants for Formation of Syn vs. Anti by the Dehydration Step  $k_{ds}/k_{da}$  and by Equilibration  $k_{as}/k_{sa}$  at 30°C

Catalyst	pH	$k_{ds}/k_{da}$	$k_{as}/k_{sa}$	$(k_{as} + k_{sa})$
				$\times 10^2 \text{ sec}^{-1}$
Dabco	9.00	0.75	1.30	6.6 <sup>a</sup>
	8.50	0.60	1.36	8.1 <sup>b</sup>
	8.00	0.78	1.36	16.9 <sup>a</sup>
		0.73	1.36	16.3 <sup>c</sup>
Phosphate	8.30	0.85 ± 0.01		
	8.10	0.87 ± 0.00		
	7.90	0.87 ± 0.04		
	7.70	0.83 ± 0.02		
Hydroxylamine	7.90	0.85		
Imidazole	7.70	0.84 ± 0.05		
	8.70	0.78		
Boric acid	9.00	0.44		
	8.70	0.37 ± 0.03		
	8.50	0.36 ± 0.01		
		0.84 ± 0.05 <sup>d</sup>		

<sup>a</sup> 0.5 M Dabco. <sup>b</sup> 0.3 M Dabco. <sup>c</sup> 0.1 M Dabco. <sup>d</sup> Ratio when methoxyamine replaces hydroxylamine as the nucleophile. Obtained from the ratio of the *O*-methyl proton resonances for the syn and anti isomers.

using a nonlinear least-squares analysis. This equation for the time dependence for the syn isomer concentration  $S$  is derived for reaction according to the mechanism given by eq 2 when the nucleophilic addition is much faster than the other steps, as observed in our experiments. In eq 3,  $S$  and  $A$  represent the syn and anti intensities, respectively, and  $B$  is  $(k_{ds} - k_{as})(k_{as} + k_{sa} - k_{ds} - k_{da})^{-1}$ . Values for  $k_{ds}$  and  $k_{da}$ , which were calculated from the syn data according to this equation, were averaged with the values calculated from the anti data according to an analogous equation. These average values are indicated in Table III. As is evident from eq 3, the same analysis provides values for  $k_{as}$  and  $k_{sa}$ . The ratio  $k_{as}/k_{sa}$  and the value of  $(k_{as} + k_{sa})$  are listed in Table III also.

Finally, some additional experiments were done to obtain information about the catalytic effect of boric acid. These experiments involved the use of methoxyamine in place of hydroxylamine. In contrast with hydroxylamine, the pH of the solution remained constant during the reaction when methoxyamine was the nucleophile and boric acid the buffer. This reaction was carried out using 0.3 M methoxyamine with boric acid at six concentrations from 0.05 to 0.5 M and a pH of 8.50. Under these conditions the ratio of syn to anti isomer from the dehydration step is 0.84 in contrast with 0.35 when hydroxylamine is used. The dehydration rate is slower for methoxyamine than for hydroxylamine. For example, when the concentration of boric acid is 0.5 M,  $k_{\text{obsd}}$  is  $8.64 \times 10^{-2} \text{ sec}^{-1}$  for hydroxylamine and  $5.23 \times 10^{-3} \text{ sec}^{-1}$  for methoxyamine. Furthermore, the catalytic effect of boric acid is much smaller for methoxyamine than for hydroxylamine. For example, at a pH of 8.50, changing the concentration of boric acid from 0.2 to 0.4 M increases the value of  $k_{\text{obsd}}$  by a factor of 1.9 for hydroxylamine compared with 1.08 for methoxyamine. In addition,  $k_{\text{obsd}}$  for methoxyamine exhibits a linear dependence on the boric acid concentration in the range 0.2 to 0.5 M in contrast with the nonlinear dependence for hydroxylamine (Figure 5). However, below a concentration of 0.1 M for boric acid, the concentration dependence for methoxyamine becomes nonlinear also.

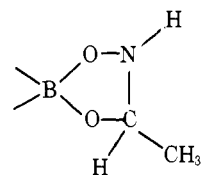
## Discussion

Because of the direct observation of the carbinolamine intermediate, it has been possible to determine the catalytic

effect of the phosphate buffer on the dehydration step. As indicated in Table I, the catalysis is mainly general acid in character; general base catalysis is negligible. These results are similar to those found for the catalytic effect of phosphate and Dabco on the dehydration of the carbinolamine formed by addition of hydroxylamine, hydrazine, or phenylhydrazinesulfonic acid to *p*-chlorobenzaldehyde.<sup>10,16</sup> In that work, general acid catalysis becomes more important as the  $\text{p}K_{\text{a}}'$  of the nucleophile increases. Consequently, our assumption that Dabco and imidazole act only as general acid catalysts for dehydration in the acetaldehyde-hydroxylamine system seems reasonable since the  $\text{p}K_{\text{a}}'$  of hydroxylamine is larger than the  $\text{p}K_{\text{a}}'$  of phenylhydrazine-*p*-sulfonic acid. As a result, the use of  $k_{\text{GA}}$  to calculate  $k_0$  at pH values for which  $k_{\text{obsd}}$  was measured at only one buffer concentration is probably acceptable for gross comparisons of  $k_0$ . Comparison of  $k_0$  values for the various buffers at identical pH values indicates a lack of agreement between phosphate and the other catalysts. For example, at pH 7.70, the concentration dependence of  $k_{\text{obsd}}$  was measured for both imidazole and phosphate, and the value of  $k_0$  for imidazole is larger than the phosphate value by over a factor of 2. Comparison of the rest of the data indicates similar differences between phosphate and the other buffers. On the other hand, the  $k_0$  values for the other catalysts show a monotonic dependence on pH. We conclude that the error is in the phosphate results and is due to large slopes in the  $k_{\text{obsd}}$  vs. concentration plots for this catalyst. Consequently the intercepts are less reliable. A detailed comparison of our results with those of other workers must be postponed until we have collected more data.

In Table III, values of the rate constants for equilibration of syn and anti isomers are given for Dabco. The rate of equilibration in the presence of each of the other buffers is substantially slower and has not been measured since each will be studied without using the flow system. The catalytic effect on equilibration caused by hydroxylamine is in between that of Dabco on the one hand and the rest of the catalysts on the other. Although it is not possible to draw any firm conclusions about the catalytic effect of Dabco on the basis of the data available, the dependence on pH suggests that the effect results from both general acid catalysis and addition of Dabco to the oxime. This type of mechanism would be consistent with the catalytic effect of hydroxylamine and the fact<sup>11</sup> that amines add to imines. Detailed equilibration studies with a variety of buffers should permit a conclusion concerning the validity of this suggested mechanism.

Finally, the results for boric acid indicate that it catalyzes the dehydration of the carbinolamine (when hydroxylamine is the nucleophile) by another process which may itself be general acid catalyzed. This process involves the addition of boric acid to the carbinolamine to form the cyclic structure



which, in turn, eliminates boric acid to form the syn and anti isomers of the oxime. General acid catalysis may be involved in either of these steps. Since boric acid is known to form analogous cyclic compounds with 1,2-diols,<sup>12</sup> the proposed structure is chemically reasonable. Support for catalysis by this process in the case of hydroxylamine is given by the following evidence. First, as indicated in Table III, the

ratio of syn to anti in the presence of boric acid is much lower than the ratio in the presence of the other catalysts. Second, while the pH changes during the dehydration reaction in the presence of boric acid, there is no pH change in the presence of the other buffers. Third, when methoxyamine is the nucleophile, there is no pH change during the addition or dehydration reaction in the presence of boric acid, and the ratio of syn to anti is 0.84, which is about the same value obtained for hydroxylamine for all buffers but boric acid. Fourth, boric acid catalysis is more pronounced for hydroxylamine than for methoxyamine. Fifth, in the concentration range 0.2 to 0.5 *M* for boric acid,  $k_{\text{obsd}}$  vs. concentration is linear for methoxyamine but nonlinear for hydroxylamine. Since the methyl group of methoxyamine can block the formation of the cyclic compound, these results are consistent with the suggested mechanism. In principle, the nonlinear dependence of  $k_{\text{obsd}}$  for hydroxylamine can be fit to a rate law which accounts for the formation of the cyclic compound and general acid catalysis by boric acid. However, the reaction is complicated by additional equilibria involving polymers of boric acid,<sup>13</sup> as indicated by the fact that the  $k_{\text{obsd}}$  vs. concentration dependence becomes nonlinear for methoxyamine when the concentration of boric acid is less than 0.1 *M*. A unique fit of the data in Figure 5 by including parameters for these equilibria, as well as the other parameters, becomes questionable in view of the number of variables that would be involved. Consequently no fit was made.

**Acknowledgment.** This work is supported in part by the Petroleum Research Fund administered by the American Chemical Society (M.C. and C.A.F.) and the National Re-

search Council of Canada (M.C. and C.A.F.). We are pleased to acknowledge helpful discussions with Professor W. P. Jencks.

## References and Notes

- (1) W. P. Jencks, "Catalysis in Chemistry and Enzymology", McGraw-Hill, New York, N.Y., 1969, Chapter 10.
- (2) W. P. Jencks, *Progr. Phys. Org. Chem.*, **2**, 63 (1964).
- (3) J. Sayer and W. P. Jencks, *J. Am. Chem. Soc.*, **95**, 5637 (1973), and references cited therein.
- (4) J. Hine and F. Via, *J. Am. Chem. Soc.*, **94**, 190 (1972), and references cited therein.
- (5) To our knowledge, the only reported observation of a reactive carbinolamine intermediate by means of ultraviolet and infrared spectroscopy has been for the reaction of various nucleophiles with the pyruvate ion; see W. P. Jencks, *J. Am. Chem. Soc.*, **81**, 475 (1959).
- (6) We have used this technique to study two other classes of reactions. See C. A. Fyfe, M. Cocivera, and S. W. H. Damji, *Chem. Commun.*, 743 (1973); M. Cocivera, C. A. Fyfe, S. P. Vaish, and H. E. Chen, *J. Am. Chem. Soc.*, **96**, 1611 (1974).
- (7) C. A. Fyfe, M. Cocivera, and S. W. H. Damji, manuscript in preparation.
- (8) S. Meiboom and D. Gill, *Rev. Sci. Instrum.*, **29**, 688 (1958).
- (9) G. Karabatsos and R. Taller, *Tetrahedron*, **24**, 3347 (1968).
- (10) (a) J. M. Sayer, M. Peskin, and W. P. Jencks, *J. Am. Chem. Soc.*, **95**, 4277 (1973); (b) J. Reiman and W. P. Jencks, *ibid.*, **88**, 3973 (1966).
- (11) Reference 2, p 506.
- (12) J. Knowlton, N. Schieltz, and D. MacMillan, *J. Am. Chem. Soc.*, **68**, 208 (1946).
- (13) N. Ingri, *Acta Chem. Scand.*, **16**, 439 (1962).
- (14) All concentrations for hydroxylamine and the various buffers are reported as total concentrations, including all states of protonation.
- (15) Under these conditions, the CH<sub>3</sub> resonance of the aldehyde is not observed and the CH<sub>3</sub> resonance of the carbinolamine is not broadened measurably compared with the case in which the base is in excess. In addition, the CH<sub>3</sub> resonance of the carbinolamine shifts down field as the initial concentration of aldehyde increases relative to the base concentration. These results indicate that the equilibrium between aldehyde and carbinolamine is rapid on the nmr time scale. Other examples in which this is not the case will be reported in subsequent papers.
- (16) In those studies, information about the dehydration step was obtained by measuring the equilibrium constant for the formation of the carbinolamine as well as the rate of hydrazone formation.

## Crystal and Molecular Structure of the Calcium Ion Complex of A23187

G. D. Smith\* and W. L. Duax

Contribution from the Medical Foundation of Buffalo, Buffalo, New York 14203. Received August 26, 1975

**Abstract:** The antibiotic A23187 is a monocarboxylic acid which has been shown to bind and transport divalent cations across natural and artificial membranes. The 1:2 calcium ion complex of the ionophore A23187 crystallizes in space group *C*2 with cell dimensions  $a = 23.715$  (7),  $b = 15.130$  (4), and  $c = 17.841$  (6) Å,  $\beta = 90.67$  (4)°, and  $Z = 4$ . The structure has been refined to a residual of 0.11. The coordination number of the calcium ion is seven. Each ionophore is bound to calcium through a carboxyl oxygen, a carbonyl oxygen, and the nitrogen of the benzoxazole ring system. The seventh position is occupied by a water molecule. Head-to-tail hydrogen bonding is observed between the two A23187 ions of the complex.

The antibiotic A23187 is a monocarboxylic acid which has been shown to bind and transport divalent cations across natural and artificial membranes.<sup>1,2</sup> By equilibrating calcium ion across the inner membrane of mitochondria, A23187 can uncouple oxidative phosphorylation.<sup>3</sup> Various biological processes which require the presence of calcium ion, such as thyroid secretion,<sup>4</sup> insulin release,<sup>5</sup> and the stimulation of the action of epinephrine on the  $\alpha$ -adrenergic receptor,<sup>6</sup> have been stimulated using this ionophore. Because of the fluorescent properties of A23187, it has been used also as a probe for divalent cations in artificial and biological membranes and to determine the mode of action of ionophore-mediated divalent cation transport.<sup>2</sup> The structure of the free acid of A23187 has been determined by chemical

methods and x-ray crystallography<sup>7</sup> and has been shown to be that illustrated in Figure 1. We report here the crystal structure of the 1:2 calcium ion complex of the ionophore.

### Experimental Section

Single crystals of the calcium ion complex of A23187 are parallelepipeds and were grown from a 95% ethanol solution containing the ionophore and calcium acetate. A single crystal measuring 0.6 × 0.6 × 0.5 mm was mounted in a glass capillary. Pertinent unit cell data are given in Table I. The intensities of 9605 independent reflections ( $\sin \theta/\lambda \leq 0.70$  Å<sup>-1</sup>) were measured on an Enraf-Nonius CAD-4 diffractometer using zirconium-filtered molybdenum radiation. No significant changes were observed in the intensities of two standard reflections which were measured after every 96 intensities were recorded. Intensities were corrected for Lorentz and